



Micromechanical modeling of elastic properties of cortical bone accounting for anisotropy of dense tissue

Laura Salguero, Fatemeh Saadat, Igor Sevostianov*

Department of Mechanical and Aerospace Engineering, New Mexico State University, Las Cruces, NM 88003, USA

ARTICLE INFO

Article history:

Accepted 18 August 2014

Keywords:

Cortical bone
Elastic properties
Microstructure
Anisotropy

ABSTRACT

The paper analyzes the connection between microstructure of the osteonal cortical bone and its overall elastic properties. The existing models either neglect anisotropy of the dense tissue or simplify cortical bone microstructure (accounting for Haversian canals only). These simplifications (related mostly to insufficient mathematical apparatus) complicate quantitative analysis of the effect of microstructural changes – produced by age, microgravity, or some diseases – on the overall mechanical performance of cortical bone. The present analysis fills this gap; it accounts for anisotropy of the dense tissue and uses realistic model of the porous microstructure. The approach is based on recent results of Sevostianov et al. (2005) and Saadat et al. (2012) on inhomogeneities in a transversely-isotropic material. Bone's microstructure is modeled according to books of Martin and Burr (1989), Currey (2002), and Fung (1993) and includes four main families of pores. The calculated elastic constants for porous cortical bone are in agreement with available experimental data. The influence of each of the pore types on the overall moduli is examined.

© 2014 Elsevier Ltd. All rights reserved.

1. Introduction

In this paper, we develop an analytical model of the effective anisotropic elastic properties of cortical bone in relation to the structure of its porous space. For this goal, we use the methodology of compliance contribution tensors first proposed by Horii and Nemat-Nasser (1983) and developed in works of Kachanov et al. (1994) and Sevostianov and Kachanov (2002). In contrast with previous modeling, we combine an account for anisotropy of dense tissue with a realistic model of microstructure that includes multiple systems of pores and canals typical for cortical bone.

Bone, as many other heterogeneous materials, is a complex arrangement, resulting in the microstructure of bone being hierarchical in nature. The microstructure at each of the levels produces a significant effect on its overall physical and mechanical properties. The structural and mechanical properties of the cortical bone, and a theoretical analysis of the connection between the structure of the porous space and the overall properties of the bone, has attracted the attention of many research groups for several decades. This interest has resulted in detailed descriptions of the structural features of bone at the macroscopic level, as well as the mechanical behavior of bone.

Morphology of the cortical bone has been well studied and the overall elastic moduli have been measured in a number of experiments starting from 1960s. Lang (1969, 1970) assumed that the cortical bone is transversely isotropic (the plane normal to Haversian canals being the plane of isotropy) and measured the five elastic constants of dry bone. Reilly and Burstein (1975), Katz et al. (1984) and Van Buskirk and Ashman (1981) measured the anisotropic moduli ultrasonically and showed that in general, cortical bone possesses orthotropic elastic properties. However stiffnesses in multiple different directions normal to Haversian canals do not vary considerably, so much so that the deviation from transversal isotropy does not exceed 10%. Direct mechanical tests performed by Zioupos et al. (1995) also confirmed closeness to transversal isotropy, although the measured values of elastic stiffnesses were smaller than the ones measured ultrasonically, probably due to inelastic deformation.

Analytically, the most common model used to represent cortical bone is the “parallel fibers” approach. Generally, it consists of two phases, the first of which is to consider a single osteon as an elongated pore, representing a Haversian canal, surrounded by lamellae of dense mineralized tissue. The second level represents the lamellae as a fiber reinforced composite of collagen fibers in hydroxyapatite matrix. In the simplest form of the parallel fiber approach, Stech (1967) analyzed the overall anisotropy of cortical bone by considering parallel cylindrical pores surrounded by layered bone tissue without any pores within the lamellae. Later, a model emphasizing the hierarchical structure of cortical bone

* Corresponding author. Tel.: +1 575 646 3322; fax: +1 575 646 6111.

E-mail address: igor@nmsu.edu (I. Sevostianov).

considered the impact on the effective elastic constants of both the porous space modeled as a set of parallel Haversian canals and the microstructure of the dense mineralized tissue, which was modeled as a fiber reinforced composite (Katz, 1981). Sevostianov and Kachanov (2000) applied the results of Eshelby's solutions for pores of different shapes to estimate the impact of the porous microstructure on the overall elastic constants of osteonal cortical bone in a micromechanical model approach. They considered a more appropriate system of pores that includes Haversian canals, osteocyte lacunae, Volkman's canals and canaliculi. The properties of the bone matrix, however were taken to be isotropic. Dong and Guo (2006) model cortical bone as a set of parallel circular Haversian canals embedded in a transversely-isotropic matrix. Later, Martínez-Reina et al. (2010) created a model that also considers cortical bone to be transversely isotropic, but expands the porosity to include canaliculi on the second level as well as takes into consideration the effects of water within the pores. The main advantage of this model that sets it apart is the ability to vary the mineral content of bone. Parnell et al. (2011) took the parallel fiber approach one step further by considering 3-phases; a polymer matrix, pores, and reinforcing particles. The Yoon and Cowin (2008a) model looks at the modulus of elasticity for a single osteonal lamellae. They view the hydroxyapatite and collagen in the bone matrix as embedded with water. This type of model agrees with many assumptions made about bone within the work presented in this paper, because the anisotropic behavior of the bone matrix is been taken into account and it demonstrates that the mechanical properties of cortical bone are highly dependent on its porosity. Nikolov and Raabe (2008) developed an analytical model that views bone as transversely isotropic. It considers only Haversian canals as the porous space within the bone microstructure. Another model employing two steps, views the lamellae as open isotropic hydroxyapatite foams. The first part represents the isotropic crystal foam as a 2-phase polycrystal, then it considers the foam as containing spherical, non-specific pores. Hellmich and Ulm, 2002 determined an appropriate model to have two main inputs; mineral volume fraction and collagen volume fraction. They went on in 2004 to expand the model to having three volume fraction inputs: hydroxyapatite, collagen, and micropore space (Hellmich et al., 2004). Fritsch et al. (2008) created a continuum mechanics model based on the works of Hellmich and Ulm (2002)

and Hellmich et al. (2004) that goes beyond porosity and stiffness relationships to resolve the material-immanent microstructures governing the overall mechanical behavior. The effect of biological liquids on mechanical properties of bone is usually taken into account with methods of poroelasticity. Yoon and Cowin (2008b) model the anisotropic poroelastic constants of a single osteon from two perspectives; drained and undrained. The undrained osteon would then have an impact on the poroelasticity from the fluid being compressed within the pores. This model allows one to distinguish between deformation-driven fluid movements (Cowin, 1999; Cowin and Sadegh, 1991) and the effect of liquid bound within closed pores (Hellmich et al., 2009). Deuerling et al. (2009) took three models for three different length scales of bone hierarchy and then applied their crystal orientation.

Many results on the mechanical properties of bone have been obtained using numerical simulations, mostly done using finite element modeling. Hogan (1992) and Crolet et al. (1993) created numerical simulations of the anisotropic moduli of cortical bone, considering only Haversian canals as elements of the porous space. Mullins et al. (2007) considered Haversian canals, Volkman's canals, and osteocyte lacunae as elements of the porous space. Dong and Guo (2004) accounted for transverse-isotropy of the matrix with the porosity associated solely with Haversian canals. Some reasons for these simplifications may be the mathematical difficulties associated with analysis of the inhomogeneities that are arbitrarily oriented in transversely-isotropic material. Despite the success of these models, they neglect potential influences from other pore types even though the contributions to the moduli of other pore types may be very strong (Currey, 1984; Martin and Burr, 1989).

To the best of our knowledge all existing analytical models of cortical bone either consider the dense bone matrix as isotropic, with any anisotropy due to oriented pores only, or they do not include a wide variety of pore type and size and account for Haversian canals only. Bone is a material with evolving microstructure, so when the partial porosities of different types of pores, the shape of these pores, and the mechanical properties of the dense tissue change with age, this lack in broader consideration by the previous works mentioned may become a serious obstacle on the way of practical applications of the micromechanical models. In the present work, we try to fill this gap. First, we account for

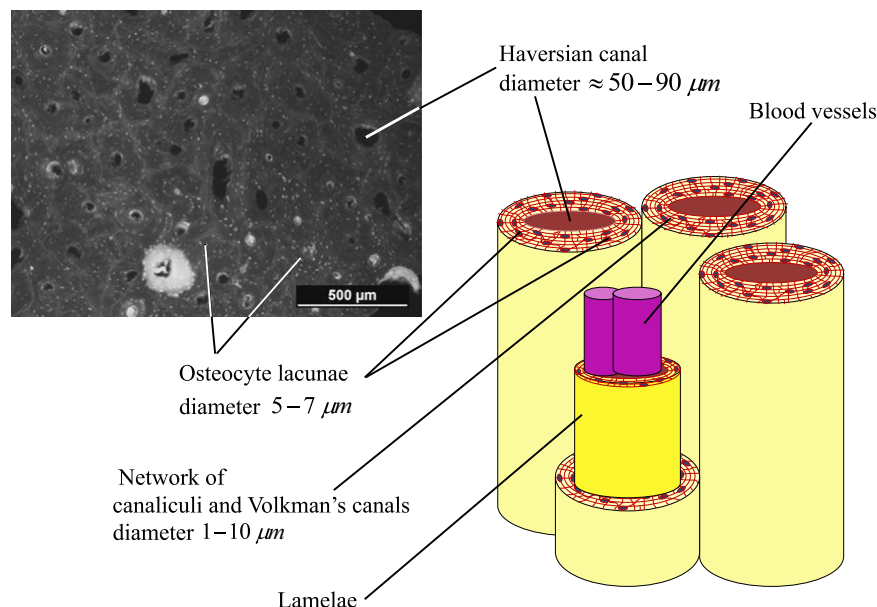


Fig. 1. Microstructure of osteonal cortical bone: SEM photomicrograph (cross-section of longitudinal cortical bovine femur) and the model used for micromechanical analysis.

anisotropy of the hard tissue that represents the composition of collagen fibrils and hydroxyapatite crystals, and second, we consider the full set of pores existing in the cortical bone and their shapes, including Haversian canals, Volkman's canals, canaliculi, and osteocyte lacunae (Currey, 1984; Martin and Burr, 1989; Fung, 1993). All these pores produce substantial effect on the overall elastic properties of cortical bone; generally they reduce the elastic stiffnesses, but this reduction is different in different directions. The extent of the reduction depends on the pore shape and its orientation with respect to the anisotropy axes of the dense tissue.

The present analysis is based on analytical results on micro-mechanics of anisotropic heterogeneous materials recently obtained by Sevostianov et al. (2005) and Saadat et al. (2012).

2. Microstructure of cortical bone

To build a suitable micromechanical model, we utilize the descriptions of the microstructure of cortical bone given in the books of Martin and Burr (1989), Currey (2002) and Fung (1993) (Fig. 1). Osteonal cortical bone is formed by osteons – cylindrical, lamellar structures 3–5 mm in length and 0.2–0.3 mm in diameter. They are surrounded by dense bone matrix, a mineralized tissue, called interstitial bone. Each osteon surrounds a Haversian canal that is around 50–90 μm in diameter and contains blood and lymph vessels and nerves. Volkman's canals – that are significantly smaller in diameter (of the order 5–10 μm) – are randomly oriented in the planes orthogonal to the Haversian canals. They provide a bridge between Haversian canals and allow blood and lymph to pass through. The lamellae in osteons contain bone cells (osteocytes) located in oblate spheroidal pores (lacunae) of diameter about 5 μm and aspect ratio 0.2 (Currey, 1962, 2002). The only way for the osteocytes to receive nutrients is by yet smaller channels (diameter of the order of 1 μm) known as canaliculi, branching orthogonally from the Haversian canals.

In our analysis, following Sevostianov and Kachanov's (1998, 2000) configuration (Fig. 2), we model cortical bone as a porous material comprised of three main systems of pores: Haversian canals, osteocyte lacunae, osteocyte canaliculi and Volkman's canals. Haversian canals are modeled as a system of parallel cylindrical pores, or strongly prolate spheroidal inhomogeneities, in which their axes of geometrical symmetry coincide with the axes of the material symmetry of the matrix (the axis of transverse-isotropy, x_3). The osteocyte lacunae, modeled as oblate spheroidal cavities, are randomly oriented in a plane of transverse-isotropy (planes normal to Haversian canals). Canaliculi and Volkman's canals are treated as a set of thin cylindrical pores, with the axis of rotation perpendicular to the axis of transverse-isotropy, which means they are lying in planes of transverse-isotropy and are randomly oriented in these planes.

The pores within the bone may vastly vary in size and shape, but their partial porosities are comparable and it is not appropriate to attribute all of the porosity to Haversian canals. Martin and Burr (1989) stated that 1 mm³ of the bone typically contains around 25,000 osteocyte lacunae with the total surface area 5 mm²/mm³, 10⁶ canaliculi with the total surface area of 160 mm²/mm³, and about 20 Haversian canals with the total surface area of 3 mm²/mm³. These numbers imply partial porosities for each of these types in the range 0.075–0.120. Since some researchers (see, for example, Cowin, 1999) reported smaller porosities, we consider, in our analysis, a relatively wide range of porosities and examine the influence of porosity on the effective elastic moduli.

As stated above, the channels and pores described contain blood and lymph vessels, nerve fibers, and living cells. The influence of these fluids and soft tissues can be neglected in the context of the overall elastic response. Indeed, elastic stiffness of

the mineralized tissue is of the order of several GPa, while Young's moduli of blood vessels are of the order of 10 MPa at pressures of 100 mm Hg, (Wesly et al., 1975). Young's moduli for the nerve tissue and for the cells are of the order of 4–10 MPa (Beel et al., 1984), and of 1 kPa, (Theret et al., 1988), correspondingly. Thus, we treat the pores as empty ones embedded in the dense tissue that represents a combination of collagen fibers (protein), and hydroxyapatite Ca₁₀(PO₄)₆(OH)₂ crystals (mineral), (Katz, 1980). Mineralized tissue possesses transversally isotropic mechanical properties, (Currey and Zioupos, 2001). In our calculations we utilized the data from Dong and Guo (2004) given in Table 1.

3. Method: compliance contribution tensor

Expression of the effective elastic properties, in terms of the microstructure, are based on the analysis of a contribution of one pore into the effective property. In other words, we evaluate each type of pore individually, then we sum the contribution of all the pores. Hence, the first problem is to identify the proper parameters of the concentration of inhomogeneities in whose terms the effective elasticity is to be expressed. Such parameters must represent individual inhomogeneities according to their actual contributions to the considered property (Kachanov and Sevostianov, 2005). These individual pore contributions for the effective elasticity are given by a tensor, called the compliance contribution tensor.

Compliance contribution tensors have been first introduced in the context of pores and cracks by Horii and Nemat-Nasser (1983) (see also detailed discussion in the book of Nemat-Nasser and Hori, 1993). Components of this tensor were calculated for 2-D pores of various shape and 3-D ellipsoidal pores in isotropic material by Kachanov et al. (1994). For the general case of elastic inhomogeneities, these tensors were introduced and calculated (for ellipsoidal shapes) by Sevostianov and Kachanov (1999, 2002). Sevostianov et al. (2005) calculated components of this tensor for a spheroidal inhomogeneity embedded in a transversely-isotropic material.

In the context of the effective elastic properties, the average, over representative volume V strain can be represented as a sum:

$$\varepsilon_{ij} = S_{ijkl}^0 \sigma_{kl}^0 + \Delta \varepsilon_{ij} \quad (1)$$

where S_{ijkl}^0 is the compliance tensor of the matrix and σ_{kl}^0 represents the Vhomogenous boundary condition (Hashin, 1983), i.e. it produces a uniform stress field within the V in the absence of the inhomogeneity, (tractions on ∂V have the form $t_{i\nu} = \sigma_{kl}^0 n_\nu$ where σ_{kl}^0 is a constant tensor); σ_{kl}^0 can be viewed as a far-field, or remotely applied, stress. The material is assumed to be a linear elastic; hence, the extra strain due to presence of inhomogeneities is a linear function of the applied stress:

$$\Delta \varepsilon_{ij} = H_{ijkl} \sigma_{kl}^0 \quad (2)$$

where H is a fourth-rank compliance contribution tensor of the inhomogeneity. In the case of multiple inhomogeneities, $\Delta \varepsilon_{ij} = H_{ijkl}^{(k)} \sigma_{kl}^0$ so that the extra compliance due to inhomogeneities is given by

$$\Delta S_{ij} = \sum H_{ijkl}^{(k)} \sigma_{kl}^0 \quad (3)$$

Remark: alternatively, one can consider the extra average stress $\Delta \sigma$ due to an inhomogeneity under given applied displacement homogeneous boundary conditions (displacements on ∂V have the form $u_{i\nu} = e^0 \cdot n_\nu$ where e^0 is a constant tensor). This defines the stiffness contribution tensor of an inhomogeneity.

The H tensor is determined by the shape and size of the inhomogeneity, as well as properties of the matrix and of the inhomogeneity material. This tensor is also affected by elastic interactions. In the non-interaction approximation, it is taken by treating the inhomogeneities as isolated ones.

Formula (3) highlights the fundamental importance of compliance, or stiffness, contribution tensors; it is these that have to be summed up and averaged in the context of the effective elastic properties. The sum:

$$\sum H^{(k)} \quad (4)$$

properly reflects compliance contributions of individual inhomogeneities and constitutes the general microstructural parameters in whose terms the effective compliance should be expressed (Kachanov and Sevostianov, 2005).

For an ellipsoidal inhomogeneity, its compliance contribution tensor is expressed in terms of tensor Q – one of two Hill's tensors (Hill, 1963; Walpole, 1966) as

$$H = \left[(S^1 - S^0)^{-1} + Q \right]^{-1}, \quad (5)$$

defined by

$$Q_{ijkl} = C_{ijmn}^0 (J_{mkl} - P_{mnr} C_{rskl}^0) \quad (6)$$

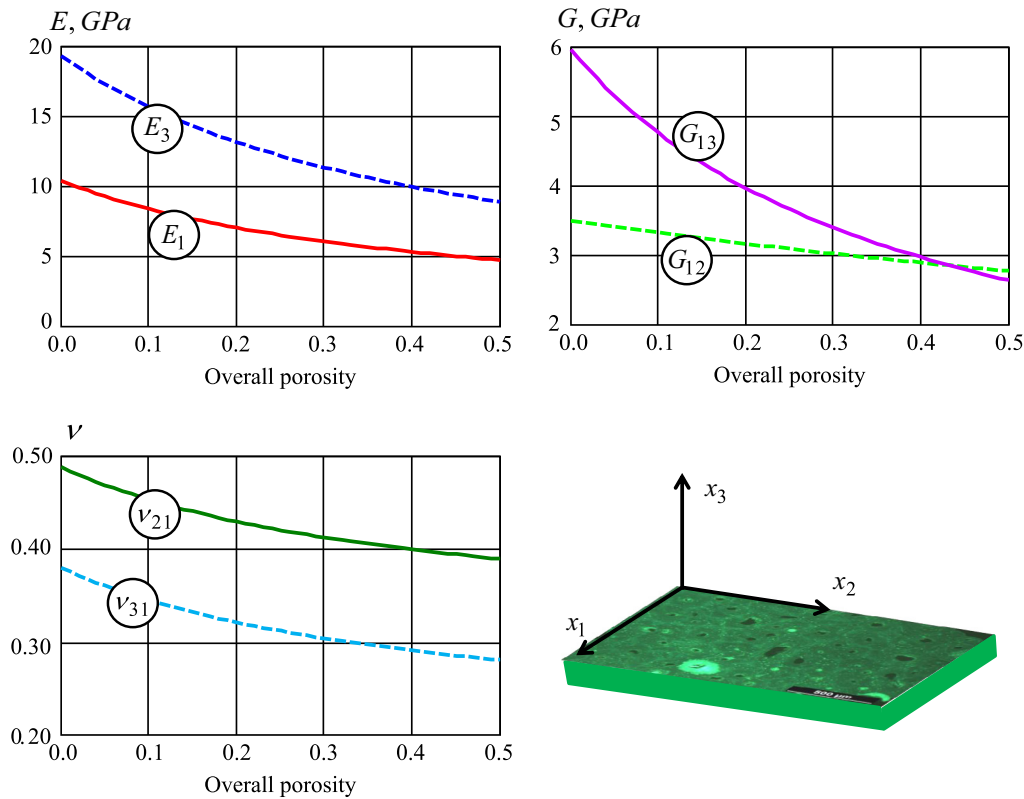


Fig. 2. Dependence of the effective elastic constants of cortical bone on the overall porosity. The sketch illustrates orientation of the Cartesian axes with respect to orientation of the osteons.

Table 1

The transversely isotropic elastic constants of cortical bone calculated based on mechanical testing done by [Dong and Guo \(2004\)](#).

Cortical bone	C_{1111} (GPa)	C_{3333} (GPa)	C_{1122} (GPa)	C_{1133} (GPa)	C_{2323} (GPa)
Experimental data	18.12	27.81	11.12	11.11	6.568

where

$$P_{mpij}(\mathbf{x}) = \frac{\partial}{\partial x_p} \int_{\Omega} \frac{\partial G_{mij}(\mathbf{x} - \mathbf{x}')}{\partial x'_i} d\mathbf{x}' \quad (7)$$

$G_{ij}(\mathbf{r})$ is Green's tensor for elasticity and parentheses in subscripts indicate symmetrization with respect to $m \leftrightarrow p$ and $i \leftrightarrow j$. Tensor P_{mpij} has the same symmetry as the tensor of elastic constants:

$$P_{ijkl} = P_{jikl} = P_{ijlk} = P_{klij} \quad (8)$$

Hence, the problem of calculating the components of \mathbf{H}_{ijkl} is reduced to the calculation of Hill's tensor. In order to evaluate the exact values for components of the compliance contribution tensor, H_{ijkl} , $P_{pqrs}^*(\mathbf{x})$ which is the Fourier transform of the tensor function of $P_{ijkl}(\mathbf{x})$, it should be integrated over unit sphere Ω_1 . In the general case of ellipsoid, if the matrix material is isotropic; tensor $P_{ijkl}(\mathbf{x})$ has the ellipsoidal symmetry and is defined by nine essential components which can be expressed in terms of elliptical integrals. It is reduced to elementary functions in the case of the spheroidal shapes. In the case of isotropic linear elastic matrix, this tensor explicitly expressed in terms of ellipsoid's geometry and Poisson's ratio of the matrix. For a spheroidal inhomogeneity embedded in a transversely-isotropic material, where axes of symmetry of the spheroid is aligned with the axis of symmetry of the matrix, the explicit closed form results are derived by [Sevostianov et al. \(2005\)](#). These relations are used in our calculation (see [Appendix A](#)).

For inhomogeneities not aligned with the symmetry axis of the matrix, like Volkman's canals and canaliculi that are normal to the axis, we use analytical approximation for components of tensor \mathbf{H}_{ijkl} following the approach proposed by [Guerrero et al. \(2007, 2008\)](#) and [Saadat et al. \(2012\)](#). We first find the best isotropic approximation for a given transversely isotropic tensor C_{ijkl} ([Fedorov, 1968](#); [Sevostianov and Kachanov, 2008](#)). It is given by tensor:

$$c\delta_{ij}\delta_{kl} + b(\delta_{ik}\delta_{jl} + \delta_{il}\delta_{kj}) \quad (9)$$

where

$$b = (3C_{iikl} - C_{iikk})/30, \quad c = (2C_{iikk} - C_{iikl})/15 \quad (10)$$

Then, we calculate the components of the compliance contribution tensor for a spheroidal pore with semi axis $a_1 = a_2 = a$, and a_3 embedded in the matrix characterized by elastic stiffnesses b and c . We are interested in the case of a strongly prolate spheroidal pore with the aspect ratio $\gamma = a_3/a \gg 1$. In this case, components of tensor \mathbf{Q}_{ijkl} are given by (see [Walpole, 1966](#)):

$$\begin{aligned} \mathbf{Q}_{1111} = \mathbf{Q}_{2222} &= 2b(4\kappa - 5\kappa f_0 - 3f_1), \quad \mathbf{Q}_{3333} = 16b(\kappa f_0 - f_1) \\ \mathbf{Q}_{1122} = \mathbf{Q}_{2211} &= 2b[4\kappa - 2 + (4 - 7\kappa)f_0 - f_1], \\ \mathbf{Q}_{1133} = \mathbf{Q}_{2233} = \mathbf{Q}_{3311} = \mathbf{Q}_{3322} &= 4b[(2\kappa - 1)f_0 + 2f_1] \\ \mathbf{Q}_{1313} = \mathbf{Q}_{2323} &= 2b(f_0 + 4f_1), \quad \mathbf{Q}_{1212} = 2b[1 - (2 - \kappa)f_0 - f_1] \end{aligned} \quad (11)$$

where the following notations are used:

$$\kappa = \frac{c+2b}{c+4b}, \quad f_0 = \frac{1-g}{2(1-\gamma^2)}, \quad f_1 = \frac{\kappa}{4(1-\gamma^2)^2}[(2+\gamma^2)g - 3\gamma^2] \quad (12)$$

$$g = \begin{cases} \frac{1}{\gamma\sqrt{1-\gamma^2}} \arctan \frac{\sqrt{1-\gamma^2}}{\gamma}, & \text{oblate shape } (\gamma < 1) \\ \frac{1}{2\gamma\sqrt{\gamma^2-1}} \ln \frac{\gamma + \sqrt{\gamma^2-1}}{\gamma - \sqrt{\gamma^2-1}}, & \text{prolate shape } (\gamma > 1) \end{cases} \quad (13)$$

So that the compliance contribution tensor for $\gamma \gg 1$ is given by (\mathbf{m} is the unit vector along the spheroid symmetry axis).

$$\begin{aligned} \mathbf{H} = \frac{V^*}{V} \frac{4b(3c+4b)}{2c+4b} &[1 - (1-2\nu^2)\mathbf{I} + 4(1-\nu^2)\mathbf{J} + (1-2\nu)(1+\nu)(\mathbf{mmmI} + \mathbf{lmmI}) \\ &- 4(1-2\nu)(1+\nu)\mathbf{mlmI} - 2\nu(1+\nu)\mathbf{mmmmI}] \end{aligned} \quad (14)$$

where $\nu = c/2c+4b$ and elastic stiffnesses c and b of the best fit material are given by (10). [Saadat et al. \(2012\)](#) examined the accuracy of this approximate method of calculation of the compliance contribution tensor. They concluded that the accuracy is the same as the accuracy of approximation (9).

4. Results and discussion: effective elastic properties of cortical bone

As a first step to determine the effective elastic properties of different individual inhomogeneities in cortical bone, we calculate

the components of the compliance contribution tensors for single inhomogeneities of different kinds. For this goal we used the properties of the dense tissue (matrix) given in Table 1 and used the approach discussed in the previous section. As mentioned above, the individual inhomogeneities are considered as empty pores since they are filled with soft materials which contribution

to the overall structural rigidity can be neglected.

$$\mathbf{H}_{ijkl} = (V^*/V)\mathbf{Q}_{ijkl}^{-1} \quad (15)$$

The results are presented in Table 2.

Total contribution of the pores into overall elastic properties of the bone can now be calculated via summation of the individual

Table 2

Components of the compliance contribution tensor for three main microstructural elements of the cortical bone.

	Single cylinder normal to the plane of isotropy (Haversian canal)	Single oblate spheroid (lacuna)	Single cylinder laying in the plane of isotropy (Volkman's canal and canaliculi)
H_{1111}	0.175	0.165	0.161
H_{3333}	0.042	0.048	0.056
H_{1122}	−0.055	−0.048	−0.049
H_{1133}	−0.010	−0.013	−0.013
H_{1212}	0.115	0.106	0.105
H_{1313}	0.073	0.069	0.069

Table 3

Components of for three systems of pores in cortical bone (p_1 , p_2 and p_3 are partial porosities of these pore systems).

	Haversian canals	Osteocyte lacunae	Volkman's canals and canaliculi
ΣH_{1111}	$0.175 p_1$	$0.165 p_2$	$0.1184 p_3$
ΣH_{3333}	$0.042 p_1$	$0.048 p_2$	$0.0995 p_3$
ΣH_{1122}	$-0.055 p_1$	$-0.048 p_2$	$-0.0119 p_3$
ΣH_{1133}	$-0.010 p_1$	$-0.013 p_2$	$-0.0310 p_3$
ΣH_{1212}	$0.115 p_1$	$0.106 p_2$	$0.0650 p_3$
ΣH_{1313}	$0.073 p_1$	$0.069 p_2$	$0.0435 p_3$

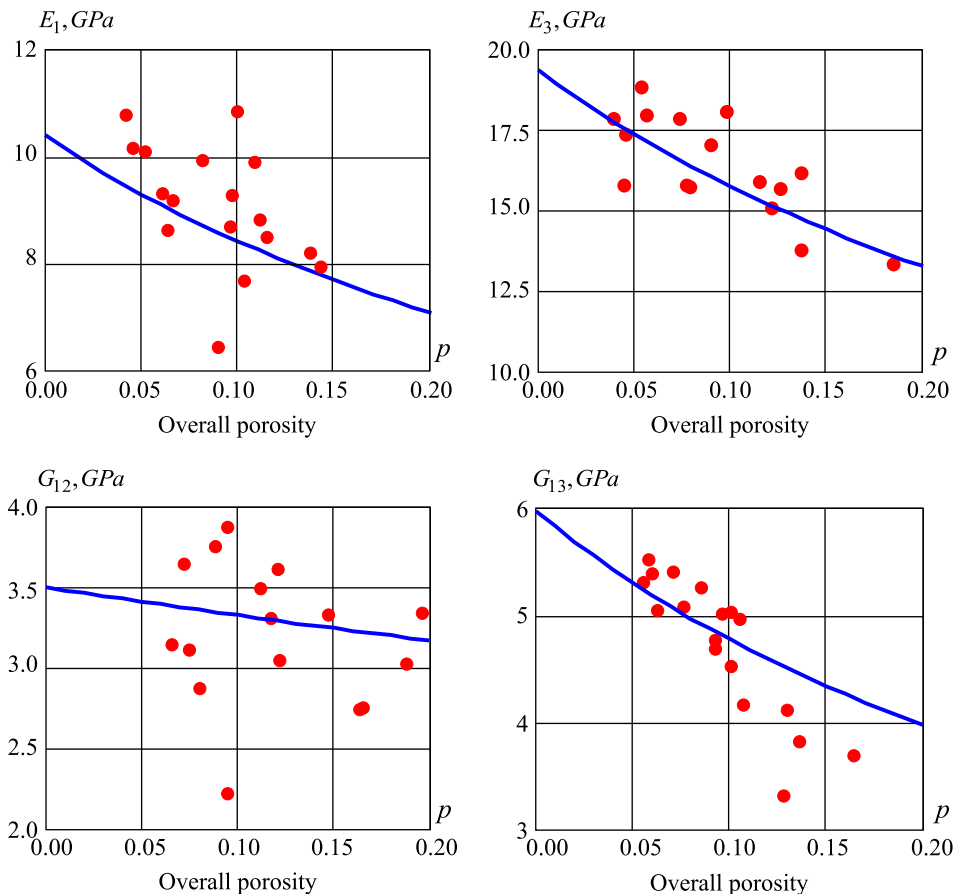


Fig. 3. Comparison of the predicted elastic moduli of the cortical bone with experimental data of Dong and Guo (2004).

pores contributions. It means that we neglect interaction between individual pores:

$$\mathbf{S}_{ijkl}^{eff} = \mathbf{S}_{ijkl}^0 + \sum \mathbf{H}_{ijkl} \quad (16)$$

where \mathbf{S}_{ijkl}^0 are the elastic compliances of the matrix (dense mineralized tissue at zero porosity) and \mathbf{S}_{ijkl}^{eff} is the effective compliance tensor. As shown by Sevostianov and Sabina (2007) the non-interaction approximation can be used with good accuracy for volume concentration of inhomogeneities up to 20%. Summation in (16) can be replaced by integration over pores orientation. The results of the calculations of $\sum \mathbf{H}_{ijkl}$ are given in Table 3.

Fig. 2 illustrates the results of our modeling. Assuming that the three types of pores: (1) Haversian canals, (2) osteocyte lacunae, and (3) Volkman's canals and canaliculi, have approximately equal partial porosities, the anisotropic effective moduli are obtained as functions of the overall porosity.

Fig. 3 provides the validation of our model – it shows the results of the comparison of predicted elastic constants (anisotropic Young's and shear moduli) with the experimental data of Dong and Guo (2004). One can see that general agreement between experimental measurements and the proposed model is reasonably good. Substantial scatter in the experimental data, however, does not allow the detailed statistical analysis.

Fig. 4 illustrates effect of variation of partial porosities on the effective elastic moduli. Partial porosities of two sets of pores are fixed as (A) 0.05 and (B) 0.10 while the third partial porosity varies. We can observe that E_1 and G_{12} are mostly affected by porosity produced by Haversian canals – solid lines show the largest slopes; E_3 and G_{13} are mostly affected by the porosity due to osteocyte

lacunae. It means, in particular, that if porosity due to other types of pores is fixed, decrease in osteocyte lacunae yields increase in overall anisotropy (increase in E_3 that is always larger than E_1). This condition, however, is not observed in real life. Usually, age-related decrease in the porosity produced by osteocyte lacunae is accompanied by appearance of resorption cavities and their growth (Parfitt, 1984).

The latter observation yields an interesting connection with the age related microstructural changes. Fig. 5 (adopted from Vashishth et al., 2000) shows the changes in the partial porosity with age. The authors particularly indicate that the number of the osteocytes exponentially decreases with age. Neglecting the size changes of individual pores, we can now estimate age-related increase in E_3 . This increase, in particular leads to higher stresses in bended bones at the same level of maximal deflection.

5. Concluding remarks

Our model provides a unique quantitative tool to describe bone while including pore shape in the determination. It demonstrated that the overall elastic constants of cortical bone were highly correlated with partial porosities, pore shapes, mechanical properties of the bone matrix and the elastic constants of the bone matrix. This implies a direct correlation between porosity and elastic properties. Changes should then be observed with age which leads to a decrease in anisotropy. This increase in porosity obviously affects the elastic properties making fracture easier and more likely. Also, from the obtained figures, it is seen that for transverse and longitudinal Young's moduli, longitudinal Poisson's

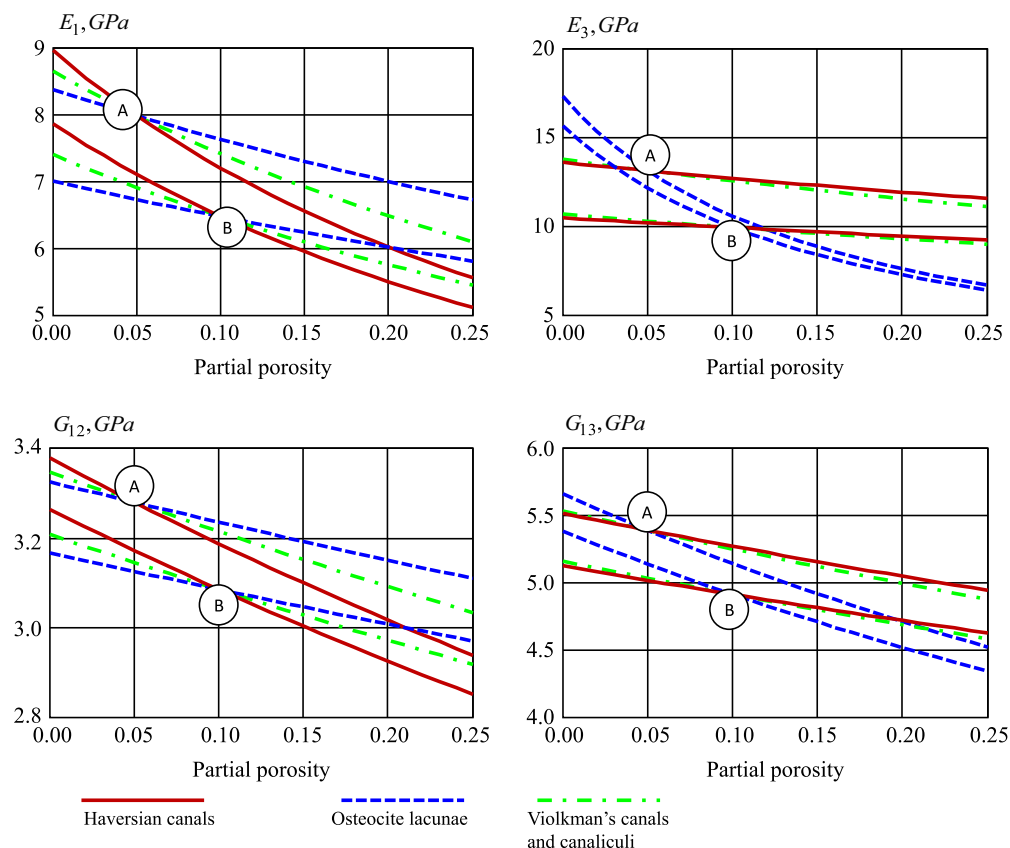


Fig. 4. The effect of the variation of the partial porosity on E_1 , E_3 , G_{12} and G_{13} : two sets of pores are fixed as (A) 0.05 and (B) 0.10 while the third partial porosity varies from 0.01 to 0.25. The slope of the curves illustrates the sensitivities of the elastic moduli to each of the partial porosities. In other words, the slope of the curves illustrates the sensitivity of the elastic moduli to each of the partial porosities.

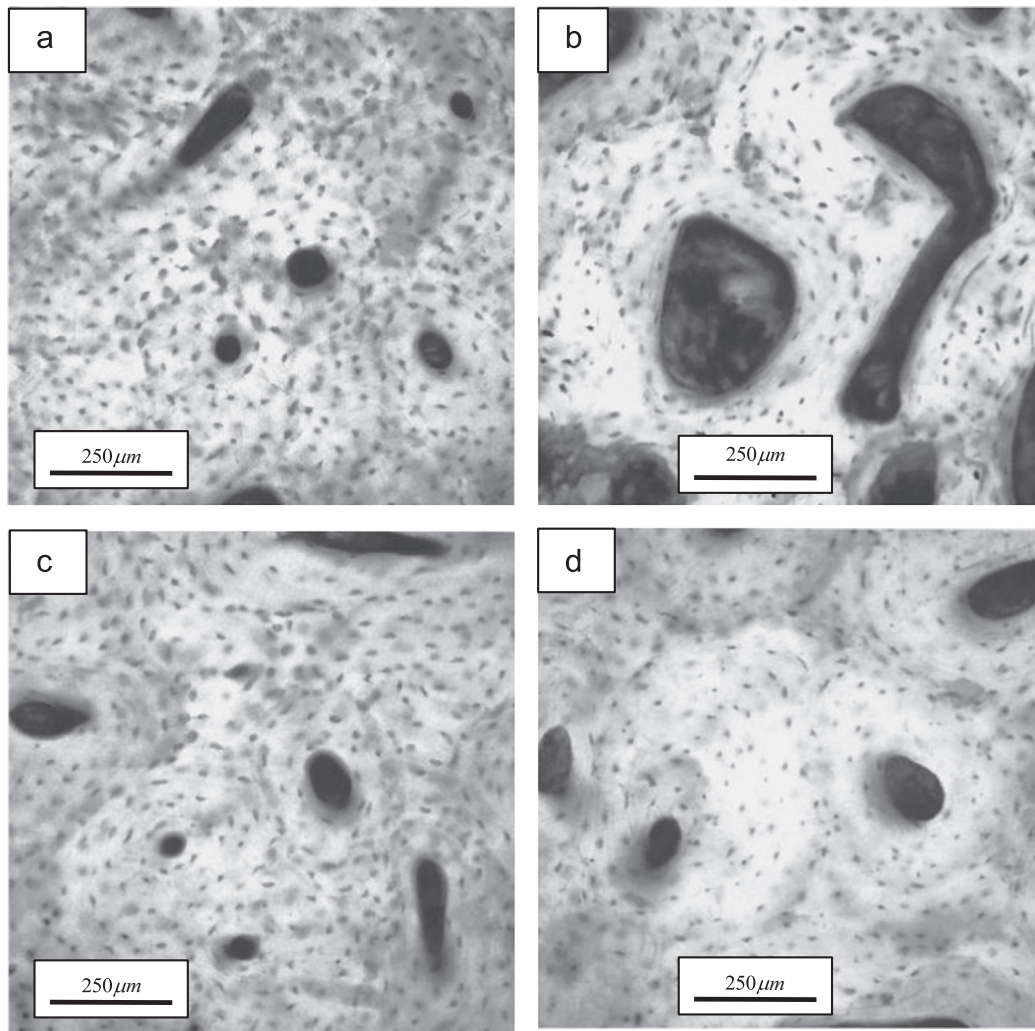


Fig. 5. Cortical bone crosssections: (a) 17 year old male, (b) 73 year old male, (c) 28 year old female, and (d) 52 year old female (from [Vashishth et al., 2000](#)).

ratio and transverse shear moduli, a very good agreement is obtained between the theoretical modeling and available experimental data. This is especially true when it is taken into account that the data is measured by different authors for elastic moduli of bone matrix and is highly variable. Despite the challenges, in the case of longitudinal shear modulus the prediction value was not consistent with the experimental results and the difference was quite significant. Since the effective properties are sensitive to the elastic properties related to the bone matrix, this disagreement might be due to considering inaccurate values for the elastic components of the bone matrix. Also, the use of partial porosity may have caused additional errors.

A possible limitation of our model is neglecting the interaction between the pores. This assumption, however, does not strongly affect the final result. As shown by [Sevostianov and Sabina \(2007\)](#) on example of a composite with transversely-isotropic matrix, non-interaction approximation produce reasonably accurate results at porosity levels up to 15–20% (depends on elastic contrast between phases). Note also that interaction effect can easily be incorporated into the model using one of many one-particle homogenization schemes (Mori-Tanaka scheme, differential scheme, Maxwell's scheme, etc., see [Sevostianov and Kachanov, 2013](#) for details). All these schemes use non-interaction approximation as the basic building block.

One of the various applications of our analysis is that the amount of mineralized tissue (hydroxyapatite content) can be

determined if the porosity is known and the overall moduli have been measured. Likewise, the porosity can be determined from the extent of mineralization and the measured elastic moduli. Recent works by [Liu et al. \(2010\)](#) have found effective methods of determining bone microstructure and porosity in vivo. Combining this imaging tool with the results here could lead to techniques to determine the progression of the aforementioned stressors that change bone and possibly an in depth study that could determine a more detailed understanding of bone remodeling and changes due to stressors.

Conflict of interest statement

The authors of this manuscript have no conflict of interest with the presented work.

Acknowledgments

This work was supported in part by a grant from the NIH Grant no. R25GM061222 and by the New Mexico Space Grant Consortium via NASA Grant no. GR0003400.

Appendix. Compliance contribution tensor of a spheroidal pore in a transversely-isotropic material

The expressions for the components of the compliance contribution tensor for spheroidal inhomogeneity in a transversely-isotropic material were calculated by [Sevostianov et al. \(2005\)](#).

We consider a spheroidal pore (or inhomogeneity that is much softer than the surrounding material) with semi-axes $a_1 = a_2 \equiv a$ and a_3 , and aspect ratio $\gamma = a_3/a$. The x_3 axis of the spheroid (\mathbf{m} being a unit vector along it) coincides with the axis of transverse isotropy of the matrix. Compliance contribution tensor can be calculated as tensor inverse to

$$\mathbf{H}_{ijkl} = \left[C_{ijmn}^0 (\mathbf{J}_{mnkl} - P_{mnrs} C_{rskl}^0) \right]^{-1} \quad (\text{A.1})$$

where Hill's tensor P_{mnrs} is calculated as

$$P_{mpij}(\mathbf{x}) \equiv \frac{\partial}{\partial x_j} \int_{\Omega} \frac{\partial G_{mij}(\mathbf{x} - \mathbf{x}')}{\partial x_j'} d\mathbf{x}'$$

We write tensor P_{ijkl} in the form:

$$P_{ijkl} = p_1 T_{ijkl}^1 + p_2 T_{ijkl}^2 + p_3 T_{ijkl}^3 + p_4 T_{ijkl}^4 + p_5 T_{ijkl}^5 + p_6 T_{ijkl}^6 \quad (\text{A.2})$$

where basic tensors T_{ijkl}^m are given by (see [Kunin, 1983](#); [Walpole, 1984](#); [Kanaun and Levin, 2008](#)):

$$\begin{aligned} T_{ijkl}^{(1)} &= \theta_{ij} \theta_{kl}, \quad T_{ijkl}^{(2)} = (\theta_{ik} \theta_{lj} + \theta_{il} \theta_{kj} - \theta_{ij} \theta_{kl})/2, \quad T_{ijkl}^{(3)} = \theta_{ij} m_k m_l, \\ T_{ijkl}^{(4)} &= m_i m_j \theta_{kl}, \quad T_{ijkl}^{(5)} = (\theta_{ik} m_l m_j + \theta_{il} m_k m_j + \theta_{jk} m_l m_i + \theta_{jl} m_k m_i)/4, \\ T_{ijkl}^{(6)} &= m_i m_j m_k m_l \end{aligned} \quad (\text{A.3})$$

with $\theta_{ij} = \delta_{ij} - m_i m_j$ and \mathbf{m} is a unit vector along the axis of transverse symmetry.

Coefficients p_i are as follows:

$$\begin{aligned} p_1 &= \frac{\pi}{2} \sum_{q=1}^3 (b_q - A_q a_q) \mathbf{J}_1^{(q)}; \quad p_2 = \frac{\pi}{2} \sum_{q=1}^3 (2b_q - A_q a_q) \mathbf{J}_1^{(q)}, \\ p_3 &= p_4 = \frac{-\pi}{2} \sum_{q=1}^3 c_q \left(\mathbf{J}_1^{(q)} - \gamma^2 A_q \mathbf{J}_2^{(q)} \right), \\ p_5 &= \pi \sum_{q=1}^3 \left[(2b_q - A_q a_q) \mathbf{J}_2^{(q)} / \gamma^2 - c_q \left(\mathbf{J}_1^{(q)} - A_q \mathbf{J}_2^{(q)} / \gamma^2 \right) + d_q \mathbf{J}_1^{(q)} \right] \\ p_6 &= 2\pi \sum_{q=1}^3 d_q \mathbf{J}_2^{(q)} / \gamma^2 \end{aligned} \quad (\text{A.4})$$

and shape factors (functions of the aspect ratio γ) are

$$\begin{aligned} \mathbf{J}_1^{(q)} &= A_q \gamma^2 \int_{-1}^1 \frac{(1-u^2) du}{[\gamma^2 + (1-\gamma^2)u^2] [A_q + (1-A_q)u^2]^{3/2}} \\ &= \lambda_q^2 \left[2 - A_q \frac{\lambda_q}{\gamma^2} \ln \left(\frac{\lambda_q + 1}{\lambda_q - 1} \right) \right] \\ \mathbf{J}_2^{(q)} &= A_q \int_{-1}^1 \frac{u^2 du}{[1 + (\gamma^2 - 1)u^2] [A_q + (1-A_q)u^2]^{3/2}} \\ &= \lambda_q^2 \left[\lambda_q \ln \left(\frac{\lambda_q + 1}{\lambda_q - 1} \right) - 2 \right] \end{aligned} \quad (\text{A.5})$$

where $\lambda_q = \gamma / \sqrt{\gamma^2 - A_q}$ and where coefficients a_i , b_i , c_i , d_i and A_i depend on elastic stiffnesses as follows:

$$\begin{aligned} a_l &= \frac{1}{\epsilon_l} \left[(C_{1212} - C_{1111})(C_{3333} - A_l C_{2323}) + (C_{1133} + C_{2323})^2 \right] \\ b_l &= \frac{1}{\epsilon_l} \left[(C_{2323} - A_l C_{1111})(C_{3333} - A_l C_{2323}) + A_l (C_{1133} + C_{2323})^2 \right] \\ c_l &= \frac{1}{\epsilon_l} (C_{1133} + C_{2323})(C_{2323} - A_l C_{1212}) \\ d_l &= \frac{1}{\epsilon_l} (C_{2323} - A_l C_{1111})(C_{2323} - A_l C_{1212}) \end{aligned}$$

$$\begin{aligned} \epsilon_l &= 4\pi C_{1111} C_{2323} C_{1212} \prod_{j=1}^3 (A_j - A_l) \\ A_l &= C_{2323} / C_{1212} \end{aligned} \quad (\text{A.6})$$

and where A_2 and A_3 are roots of the quadratic equation ([Elliott, 1948](#)).

$$C_{1111} C_{2323} A^2 + (C_{1133}^2 + 2C_{1133} C_{2323} - C_{1111} C_{3333}) A + C_{2323} C_{3333} = 0 \quad (\text{A.7})$$

In particular for *strongly prolate spheroidal inhomogeneity* ($\gamma \rightarrow \infty$),

$$\mathbf{J}_1^{(q)} = 2; \quad \mathbf{J}_2^{(q)} / \gamma^2 \rightarrow 0 \quad (\text{A.8})$$

and

$$\begin{aligned} \sum_{q=1}^3 b_q &= \frac{1}{2\pi C_2}; \quad \sum_{q=1}^3 c_q = 0; \quad \sum_{q=1}^3 d_q = \frac{1}{\pi C_5}; \\ \sum_{q=1}^3 (b_q - A_q a_q) &= \frac{1}{2\pi(2C_1 + C_2)} \end{aligned} \quad (\text{A.9})$$

Substitution of (A.8) into (A.4) leads to the following coefficients of representation of tensor \mathbf{P} in the standard tensor basis:

$$\begin{aligned} p_1^0 &= \frac{1}{2(2C_1 + C_2)}; \quad p_2^0 = \frac{1}{2(2C_1 + C_2)} + \frac{1}{2C_2}; \\ p_5^0 &= 2/C_5; \quad p_3^0 = p_4^0 = p_6^0 = 0 \end{aligned} \quad (\text{A.10})$$

In particular, if the matrix material is *isotropic*, we recover a known result ([Sevostianov and Kachanov, 1999](#)).

$$P_{1111} = P_{2222} = \frac{4-3\kappa}{8\mu}, \quad P_{1122} = P_{2211} = \frac{-\kappa}{8\mu}, \quad P_{1212} = \frac{2-\kappa}{8\mu},$$

$$P_{1313} = P_{2323} = \frac{1}{8\mu}$$

$$P_{3333} = P_{1133} = P_{2233} = P_{3311} = P_{3322} = 0$$

where μ is the shear modulus and κ is connected with Poisson's ratio ν as $\kappa = 1/[2(1-\nu)]$.

References

- Beel, J.A., Grosz, D.E., Luttges, M.W., 1984. Alterations in the mechanical properties of peripheral nerve following crush injury. *J. Biomech.* 17, 185–193.
- Cowin, S.C., Sadeq, A.M., 1991. Non-interacting modes for stress, strain and energy in hard tissue. *J. Biomech.* 24, 859–867.
- Cowin, S.C., 1999. Bone poroelasticity. *J. Biomech.* 32, 217–238.
- Crolet, J.M., Aoubiza, B., Meunier, A., 1993. Compact bone: numerical simulation of mechanical characteristics. *J. Biomech.* 26, 677–687.
- Currey, J.D., 1962. Stress concentrations in bone. *Quarterly J. Microsc. Sci.* 103, 111–133.
- Currey, J.D., 1984. *The Mechanical Adaptations Of Bone*. Princeton University Press, Princeton, New Jersey.
- Currey, J.D., Zioupos, P., 2001. The effect of porous microstructure on the anisotropy of bone-like tissue: a counter example. *J. Biomech.* 34, 707–710.
- Currey, J.D., 2002. *Bones: Structure and Mechanics*. Princeton University Press, New York, pp. 12–21.
- Dong, X.N., Guo, X.E., 2004. The dependence of transversely isotropic elasticity of human femoral cortical bone on porosity. *J. Biomech.* 37, 1281–1287.
- Dong, X.N., Guo, X.E., 2006. Prediction of cortical bone elastic constants by a two-level micromechanical model using a generalized self-consistent method. *J. Biomech. Eng.* 128, 309–316.
- Deuring, Justin M., Yue, Weimin, Espinoza Orias, Alejandro A., Roeder, Ryan K., 2009. Specimen-specific multi-scale model for the anisotropic elastic constants of human cortical bone. *J. Biomech.* 42, 2061–2067.
- Elliott, H.A., 1948. Three-dimensional stress distributions in hexagonal aeolotropic crystals. *Proc. Camb. Phil. Soc.* 44, 522–533.
- Fedorov, F., 1968. *Theory of Elastic Waves in Crystals*. Plenum Press, New York.
- Fritsch, A., Dormieux, L., Hellmich, C., Sanahuja, J., 2008. Mechanical behavior of hydroxyapatite biomaterials: an experimentally validated micromechanical model for elasticity and strength. *Wiley Inter Science* 10.1002/jbm.a.31727.
- Fung, Y.C., 1993. *Biomechanics: Mechanical Properties of Living Tissues*. Springer, New York.
- Guerrero, F., Sevostianov, I., Giraud, A., 2007. On an arbitrarily oriented crack in a transversely-isotropic medium. *Int. J. Fract.* 148, 273–279.
- Guerrero, F., Sevostianov, I., Giraud, A., 2008. On an arbitrarily oriented crack in a transversely-isotropic medium. *Int. J. Fract.* 153, 169–176.

- Hashin, Z., 1983. Analysis of composite materials. *J. Appl. Mech.* 50, 481–505.
- Helmich, C., Ulm, F.J., 2002. Micromechanical model for ultrastructural stiffness of mineralized tissues. *J. Eng. Mech.* 128, 898–908.
- Helmich, C., Ulm, F.J., Dormieux, L., 2004. Can the diverse elastic properties of trabecular and cortical bone be attributed to only a few tissue-dependent phase properties and their interactions? Arguments from a multiscale approach. *Biomech. Model. Mechanobiol.* 2, 219–238.
- Helmich, C., Celundova, D., Ulm, F.J., 2009. Multiporoelasticity of hierarchically structured materials micromechanical foundations and application of bone. *J. Eng. Mech. ASCE* 135, 382–394.
- Hill, R., 1963. Elastic properties of reinforced solids: some theoretical principles. *J. Mech. Phys. Solids* 11, 357–372.
- Hogan, H.A., 1992. Micromechanics modeling of haversian cortical bone properties. *J. Biomech.* 25, 549–556.
- Horii, H., Nemat-Nasser, S., 1983. Overall moduli of solids with microcracks: load-induced anisotropy. *J. Mech. Phys. Solids* 31, 155–171.
- Kachanov, M., Tsukrov, I., Shafiro, B., 1994. Effective moduli of solids with cavities of various shapes. *Appl. Mech. Rev.* 47, S151–S174.
- Kachanov, M., Sevostianov, I., 2005. On quantitative characterization of microstructures and effective properties. *Int. J. Solids Struct.* 42, 309–336.
- Kanaun, S.K., Levin, V.M., 2008. Self-Consistent Methods for Composites (Static Problems). 1. Springer, Berlin.
- Katz, J.L., 1980. Anisotropy of Young's modulus of bone. *Nature* 283, 106–107.
- Katz, J.L., 1981. Composite material models for cortical bone. In: Cowin, S.C. (Ed.), *Mechanical Properties of Bone*, 45. ASME, New York, pp. 171–184.
- Katz, J.L., Yoon, H.S., Lipson, S., Maharidge, R., Meunier, A., Christel, P., 1984. The effects of remodeling on the elastic properties of bone. *Calcif. Tissue Int.* 36, S31–S36.
- Kunin, I.A., 1983. *Elastic Media With Microstructure*. Springer Verlag, Berlin.
- Lang, S.B., 1969. Elastic coefficients of animal bone. *Science* 3, 165–287.
- Lang, S.B., 1970. Ultrasonic method for measuring elastic coefficients of bone and results on fresh and dried bovine bones. *IEEE Trans. Biomed. Eng.* 17, 101–105.
- Liu, X.S., Zhang, X.H., Sekhon, K.K., Adams, M.F., McMahon, D.J., Bilezikian, J.P., Shane, E., Guo, X.E., 2010. High-resolution peripheral quantitative computed tomography can assess microstructural and mechanical properties of human distal tibial bone. *J. Bone Miner. Res.* 25, 746–756.
- Martin, R.B., Burr, D.B., 1989. *Structure, Function and Adaptation of Compact Bone*. Raven Press, New York.
- Martínez-Reina, J., Domínguez, J., García-Aznar, J.M., 2010. Effect of porosity and mineral content on the elastic constants of cortical bone: a multiscale approach. *Biomech. Model. Mechanobiol.* 10, 309–322.
- Mullins, P., McGarry, J.P., Bruzzi, M.S., McHugh, P.E., 2007. Micromechanical modeling of cortical bone. *Comput. Methods Biomech. Biomed. Eng.* 10, 159–169.
- Nikolov, S., Raabe, D., 2008. Hierarchical modeling of the elastic properties of bone at submicron scales the role of extrafibrillar mineralization. *Biophys. J.* 94, 4220–4232.
- Parfitt, A.M., 1984. Age-related structural changes in trabecular and cortical bone: cellular mechanisms and biomechanical consequences. *Calcif. Tissue Int.* 36, S123–S128.
- Parnell, W.J., Vu, M.B., Grimal, Q., Naili, S., 2011. Analytical methods to determine the effective mesoscopic and macroscopic elastic properties of cortical bone. *Biomech. Model. Mechanobiol.* 11, 883–901.
- Reilly, D.T., Burstein, A.H., 1975. The elastic and ultimate properties of compact bone tissue. *J. Biomech.* 8, 393–405.
- Saadat, F., Sevostianov, I., Giraud, A., 2012. Approximate representation of a compliance contribution tensor for a cylindrical inhomogeneity normal to the axis of symmetry of transversely isotropic material. *Int. J. Fract.* 174, 237–244.
- Sevostianov, I., Kachanov, M., 1999. Compliance tensors of ellipsoidal inclusions. *Int. J. Fract.* 96, L3–L7.
- Sevostianov, I., Kachanov, M., 1998. On the relationship between microstructure of the cortical bone and its overall elastic properties. *Int. J. Fract.* 92, L3–L8.
- Sevostianov, I., Kachanov, M., 2000. Impact of the porous microstructure on the overall elastic properties of the osteonal cortical bone. *J. Biomech.* 33, 881–888.
- Sevostianov, I., Kachanov, M., 2002. Explicit cross-property correlations for anisotropic two-phase composite materials. *J. Mech. Phys. Solids* 50 (2002), 253–282.
- Sevostianov, I., Kachanov, M., 2008. On approximate elastic symmetries and elliptic orthotropy. *Int. J. Eng. Sci.* 46, 211–223.
- Sevostianov, I., Kachanov, M., 2013. Non-interaction approximation in the problem of effective properties. In: Kachanov, M., Sevostianov, I. (Eds.), *Effective Properties of Heterogeneous Materials*. Springer, Berlin, pp. 1–96.
- Sevostianov, I., Yilmaz, N., Kushch, V., Levin, V., 2005. Effective elastic properties of matrix composites with transversely-isotropic phases. *Int. J. Solids Struct.* 42, 455–476.
- Sevostianov, I., Sabina, F., 2007. Cross-property connections for fiber reinforced piezoelectric materials. *Int. J. Eng. Sci.* 45, 719–735.
- Stech, E.L., 1967. A descriptive model of lamellar bone anisotropy. In: Byars, E.F. (Ed.), *Biomechanics Monographs*. ASME, New York (chapter 3).
- Theret, D.P., Levesque, M.J., Sato, M., Nerem, R.M., Wheeler, L.T., 1988. The application of a homogeneous half-space model in the analysis of endothelial cell micropipette measurements. *ASME J. Biomech. Eng.* 110, 190–199.
- Van Buskirk, W.C., Ashman, R.B., 1981. The elastic moduli of bone. *Mechanical properties of bone (AMD)*. In: Cowin, S.C. (Ed.), 36. ASME, New York, pp. 131–143.
- Vashishth, O., Verborgt, O., Divine, G., Schaffler, M.B., Fyhrie, D.P., 2000. Decline in osteocyte lacunar density in human cortical bone is associated with accumulation of microcracks with age. *Bone* 26 (4), 375–380.
- Walpole, L.J., 1966. On bounds for overall elastic moduli of inhomogeneous systems: Part I. *J. Mech. Phys. Solids* 14, 151–162.
- Walpole, L.J., 1984. Fourth-rank tensors of the thirty-two crystal classes: multiplication tables. *Proc. R. Soc. Lond. A* 391, 149–179.
- Wesly, R.L.R., Vaishnav, R.N., Fuchs, J.C.A., Patel, D.J., Greeneld Jr., J.C., 1975. Static linear and nonlinear elastic properties of normal and arterIALIZED venous tissue in dog and man. *Circ. Res.* 37, 509–520.
- Yoon, Y.J., Cowin, S.C., 2008(). An estimate of anisotropic poroelastic constants of an osteon. *Biomech. Model. Mechanobiol.* 7, 13–26.
- Yoon, Y.J., Cowin, S.C., 2008(). The estimated elastic constants for a single bone osteonal lamella. *Biomech. Model. Mechanobiol.* 7, 1–11.
- Ziopoulos, P., Currey, J.D., Mirza, M.S., Barton, D.C., 1995. Experimentally determined microcracking around a circular hole in a flat plate of bone: comparison with predicted stresses. *Philos. Trans. R. Soc. Lond. B* 347, 383–396.